IEEE Access
Multidisciplinary ⋮ Rapid Review ⋮ Open Access Journal

Received 21 November 2022, accepted 27 November 2022, date of publication 30 November 2022, date of current version 6 December 2022.

Digital Object Identifier 10.1109/ACCESS.2022.3225653

RESEARCH ARTICLE

Inter-Radar Interference Analysis Based on L and S Band Propagation Models and Radar Beam-Scanning Scenarios

HYUNGJUNG KIM[1], YOUNGDAM KIM[2], MINSOO KANG[1], SANGIN CHO[1], AND BYUNGKWAN KIM[3], (Member, IEEE)

[1]Radio and Satellite Research Division, Electronics and Telecommunications Research Institute, Daejeon 34129, South Korea
[2]Department of Electrical Engineering, Chungnam National University, Daejeon 34134, South Korea
[3]Department of Radio and Information Communications Engineering, Chungnam National University, Daejeon 34134, South Korea

Corresponding author: Byungkwan Kim (byungkwan.kim@cnu.ac.kr)

This work was supported in part by the Institute of Information & Communications Technology Planning & Evaluation (IITP) funded by the Korean Government [Ministry of Science and Information and Communications Technology (MSIT)] through the Development of Core Technology for Efficient Radar Spectrum Use under Grant 2020-0-00878, and in part by the Regional Innovation Strategy (RIS) through the National Research Foundation of Korea (NRF) funded by the Ministry of Education (MOE) under Grant 2021RIS-004.

ABSTRACT This paper presents an overview and novel method on inter-radar interference analysis based on propagation models and radar beam-scanning scenarios. Many studies on radar interference have provided proper methodologies and recommendations for system safety, coexistence, and higher spectrum utilization. However, the propagation models and radar beam-scanning scenarios have not given detail consideration because they usually focus on the proposed interference mitigation techniques. This paper provides a statistical interference analysis method to understand selection of propagation model and various beam-scanning scenarios on the radar interference. The time, duration, probability of the worst-case interference and expected performance degradation is presented statistically. From the simulation result, the maximum gain alignment under 1 degree between two radar occurs with 1.82×10^{-5} probability in an example scenario. The proposed simulation and analysis method can help to derive radar operational parameters for interference mitigation and efficient spectrum utilization.

INDEX TERMS Radar interference, radar simulation, electromagnetic propagation.

I. INTRODUCTION

Most radiodetermination and radiolocation radar systems operate under limited bandwidths and licenses because a high-power and pulsed transmitted signal can significantly damage other wireless transceiver systems. However, the demand for high-performance and wide-coverage radar systems is increasing continuously because of new threats and events in the real world, such as unmanned aerial vehicles for airport surveillance radar and unexpected torrential rains for weather radar. Increasing the performance and coverage of a radar system increases its transmission power and bandwidth, which may interfere with other radio systems. To prevent interference between various radio systems, criteria and procedures are presented to analyze and predict for the coexistence of various radio services.

For radiodetermination radar system, ITU-R M.1461-2 [1] recommended procedures for determining the potential interference and it noted that the effect of pulsed interference is difficult to quantify and strongly dependent on the receiver/processor design and operating mode. ITU-R M.2136 [2] provided theoretical analysis and test results pertaining to the determination of relevant interference protection criterias (IPC) of ground-based meteorological radar with the key objective of establishing the maximum interference level. ITU-R M.1849-2 [3] discussed the effects of interference on meteorological radar and developed related IPCs. In addition, a theoretical analysis was presented on the effect of continuous wave (CW) and pulsed interference upon weather radar products as a function

The associate editor coordinating the review of this manuscript and approving it for publication was Chan Hwang See.

of the interference-to-noise ratio (I/N). These criteria and procedures need proper selection of radio propagation model for accurate analysis.

Radio propagation model determines the path loss of a signal between two points, considering various environmental factors such as the terrain, the weather, and the propagation conditions. For example, Moraitis et al. [4] analyzed interference using ITU-R P.452 model for LTE network and air traffic control radar for partially light urban, sea, and open area. Similarly, [5], [6], [7], [8] utilized P.452 model by considering operating frequency, terrain type and time-percentage of the case. [7], [9] used ITU-R P.2001 because of delta Bullington diffraction model, and [10], [11] adopted Irregular Terrain Model (ITM). In case of urban area, Extended Hata propagation model are used in [12] and [13].

However, as noted in [1], [2], and [3], The interference signal power is not determined by only the propagation model and path loss. To accurately estimate the victim's interference signal, the following parameters are required: The transmission power of the interferer, antenna scan patterns of the interferer and victim, frequency-dependent rejection (FDR), and propagation loss between them. The transmission power and FDR are determined values, but the propagation loss may vary between models and the antenna scan patterns are easily adjusted by the operator.

In this context, interference studies provided limited results with a single propagation model and limited antenna scan scenario. For example, in the coexistence study between LTE-U and shipborne radar, the authors used extended Hata model and assumed that antenna to be fixed in [13]. However, in [14], free space path loss model is adopted when analyzing interference between LTE-U and rotating shipborne radar. Recent radar interference studies [15], [16], [17] analyzed on performance degradation of victim system, and the interference power is assumed to be enough to exceed the protection level. In [18], radar-radar coexistence is analyzed with free space path loss model and a synchronized scanning scenario. Similarly, passive bistatic radar detection performance is analyzed with fixed antenna patterns and free space path loss model in [19]. Therefore, it is difficult to verify the importance and difference of propagation models or beam scanning scenarios from a radar literature.

The motivation of this paper is to provide comparative interference analysis method and result based on various propagation models and scenarios for inter-radar interference cases. Interference analysis with different propagation model can provide environmental understanding, and with beam-scanning scenario, it can be utilized to determine radar operational parameters.

The main contribution of this study can be presented as follows:

- An inter-radar interference simulation and analysis method is presented to examine the significance of propagation models and radar beam scanning scenario.
- Interference analysis with various propagation models will help to understand and select proper propagation model for the scenario.
- The power, duration, time and probabilities of interference signal with given criteria can be analyzed statistically.
- The statistical results of interference analysis with various scenarios will help to determine radar operational parameters and scanning method.
- The method proposed in this paper is applicable to radar systems in other frequency bands such as X-band and C-band with other propagation models.

The rest of the paper is organized as follows. Section 2 presents propagation models for inter-radar interference analysis as well as path loss examples. Section 3 presents interference analysis methods and simulation results for different radar beam-scanning scenarios. Finally, Section 4 concludes the paper.

TABLE 1. L and S bands radio propagation models.

Model	Frequency (GHz)	Distance (km)	Link Type [1]	Purpose
P.452	0.1∼ 50	∼10000	G-G	Interference
P.528	0.125∼15.5	Any	G/S(A)-S(A)	Radiolocation
P.2001	0.03∼50	3∼1000	G-G	General
P.617	0.03∼	100∼1000	G-G	Radio-relay
P.530	Any	Any	G-G	LoS Link
ITM	0.02∼20	1∼2000	G-G	General

[1] G: Ground, S: Satellite, A: Aeronautical

II. PROPAGATION MODELS FOR INTER-RADAR INTERFERENCE ANALYSIS

This section presents considerations for propagation models for inter-radar interference analysis. As mentioned in Section I, the choice of the propogation model and parameter selections are crucial in the radar interference problem. We reviewed the propagation models for L and S band radar systems and selected the proper models for the interference analysis.

A. PROPAGATION MODEL CANDIDATES

Table 1 lists the propagation models considered for inter-radar interference analysis in the L and S bands from 1 to 4 GHz: ITU-R P.452, ITU-R P.528, ITU-R P.617, ITU-R P.530, ITU-R P.2001, and ITM (Longley-Rice). The major criteria considered for the selection of propagation models were the applicable frequency, distance, link type, purpose and services, and statistical input data, such as the time percentage and variability. We limited the scope of the analysis to fixed radars on the ground, the L and S frequency bands, and inter-radar interference only. These limitations excluded P.528, P.617, and P.530. P.528 was not compatible because this model considered radars on a moving platform such as aircraft or ships. P.617 focuses on trans-horizon radio transmission path losses, which are from diffraction and tropospheric scatter rather than topographic data. This model

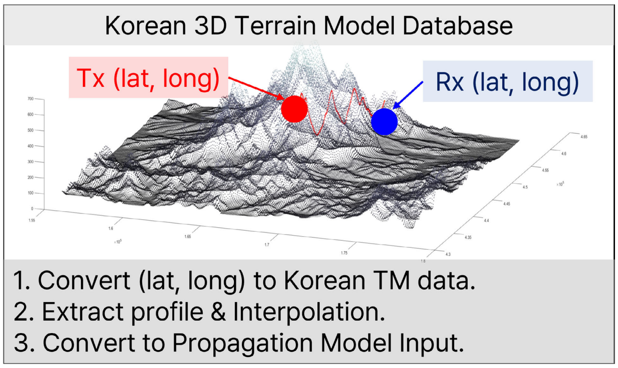

FIGURE 1. Three steps of topographic data generation in South Korea for path loss calculation.

is only applicable to some over-the-horizon radars and not to general L and S band radar systems. Similarly, P.530 is designed only for line-of-sight (LOS) systems, but inter-radar interference can occur between non-line-of-sight (NLOS) systems. P.452, P.2001, and ITM were suitable propagation models for this study considering their design objectives and environmental input data.

B. PATH LOSS CALCULATION IN SOUTH KOREA

The selected propagation models requires the latitude and longitude of the Tx and Rx stations and the path profile between the two points to calculate path loss. In order to calculate the path loss using these three models, the path profile format is defined as the elevation (m) for the distance (km) away from the transmitting station. However, the TM data is a data format for accurately modeling the topography in a grid structure in Korea, not a latitude-longitude coordinate system. Therefore, it is required to match the TM topographic data with the latitude-longitude coordinate system. This process corresponds to first and second block of Fig. 3.

1) PROFILE EXTRACTION IN SOUTH KOREA

South Korea topographic database are provided by the National Geographic Information Institute of Korea and released to the public in 2014. This database uses the transverse Mercator (TM) coordinate system and has a resolution of 90 m. The database also provides statistical information for reference and has a maximum error of −23.46 m, minimum error of 0.00 m, mean error of −0.70 m, and standard deviation of 4.77 m. Fig. 1 shows the method used for terrain profile extraction, which comprises three steps: (1) converting the latitude/longitude of the transmitted (Tx) and received (Rx) data into a coordinate system that conforms to the Korean TM data format; (2) forming a straight line connecting two points on the TM data and extracting the profile from the desired number of samples using interpolation; and (3) expressing the extracted profile in one dimension as a height versus distance matrix.

TABLE 2. Calculated path loss results for four cases in South Korea. The time variability of ITM is set as 0.01.

Model	Time Percentage p	Case 1	Case 2	Case 3	Case 4
Friis	N/A	139.08	131.81	142.12	141.70
P.452	0.01	130.10	124.80	189.64	187.56
	0.5	134.51	129.05	194.06	191.04
P.2001	0.01	126.15	124.79	187.15	188.86
	0.5	131.45	131.46	193.79	193.24
ITM	N/A	134.22	127.61	216.64	197.46

Fig. 2 shows the profile extraction results for four arbitrarily selected cases in Korea. For cases 1 and 2, LOS profiles were selected. For cases 3 and 4, NLOS profiles were selected. Cases 1∼4 had distances d of 76, 33, 108, and 103 km, respectively.

2) PATH LOSS RESULTS AND DISCUSSIONS

For the propagation models, the basic inputs were entered as recommended for the corresponding region in Korea. The most important input variables for path loss calculation are the time percentage p and profile. The time percentage is defined as the proportion of average years in which the predicted basic transmission loss is not exceeded, and it was set to two values: 0.01 and 0.5. The path loss was calculated by using the profiles of the four cases shown in Fig. 2. Table 2 present the calculated path losses for the profiles.

The path loss tended to increase as the time percentage increased. A high time percentage indicates a received signal power that can be obtained with a high probability most of the time. In general, the propagation level fluctuates because of several factors such as fading and weather. Owing to the temporal variability of the received signal power, a low received signal power is generally obtained with a wide time domain. In other words, a wide time domain corresponds to a high time percentage. Therefore, a high path loss corresponds to a low received signal power. A low time percentage corresponds to the opposite of the situation explained above.

P.452 and P.2001 are very similar models, and they were designed to give the worst-case path loss for interference analysis. In contrast, ITM provides a more theoretical path loss for wireless links that accurately reflects factors such as the reflection and diffraction of electromagnetic waves due to topographical factors. Therefore, P.452 and P.2001 always gave a lower path loss for all cases than ITM. A low path loss means a high received signal power, which corresponds to the worst-case interference for the victim radar. In addition, for ITM, the path loss became very high in the NLOS cases. This means that ITM calculated the path loss of the terrain profile based on the electromagnetic diffraction theory. In both cases 3 and 4, a very complex mountainous terrain was between the radio links, and only a diffraction path was created. These diffracted waves caused very large propagation attenuation.

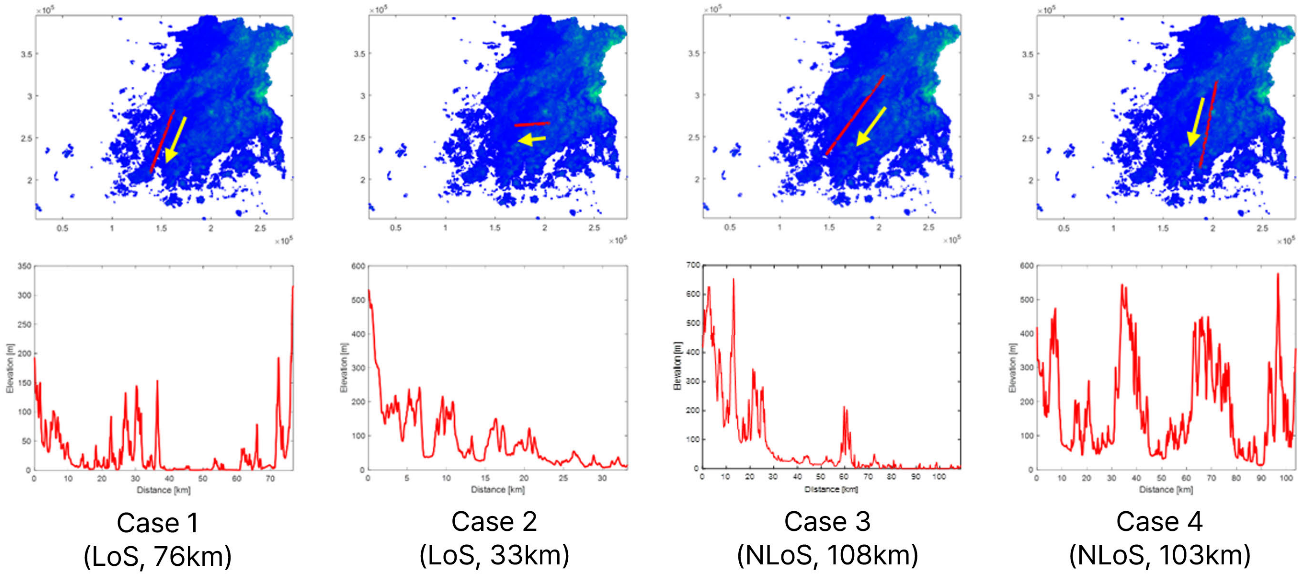

FIGURE 2. Profile extraction results in four cases including LOS and NLOS cases.

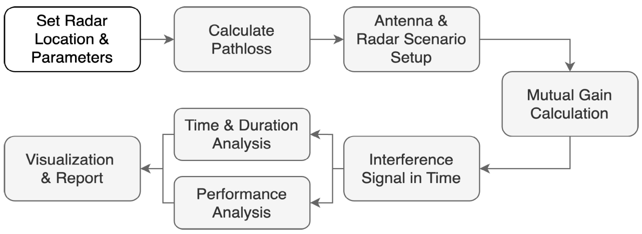

FIGURE 3. The block diagram of proposed interference simulation method.

III. INTER-RADAR INTERFERENCE ANALYSIS

A. METHODOLOGY

The proposed analysis starts from a recommendation that describes the procedure to estimate the interference power level between two radars from ITU-R M.1461-1 [1]. The recommendation describes the received interference power at victim radar with following equation:

$$I = P_T + G_T + G_R - L_T - L_R - L_P - FDR \tag{1}$$

where P_T is the transmitted power from the interferer radar. G_T is the antenna gain of the interferer radar, and G_R is the antenna gain of the victim radar. L_T is the insertion loss of the interferer radar, L_R is the insertion loss of the victim radar, and L_P is the propagation loss calculated previously. FDR is determined by the receiver selectivity. ITU-R SM.337 [20] defines FDR as follows.

$$FDR = 10\log_{10}\left(\frac{\int_{-\infty}^{\infty}\Phi(f)df}{\int_{-\mathrm{inf()}ty}^{\infty}\Phi(f)\Psi(f-\Delta f)df}\right) \tag{2}$$

The proposed method focuses on the fact that the interference signal power varies with time because both the interferer and victim radars rotate antennas independently. The rotations of the interferer and victim radars change their effective antenna gains for the interference signal path as a function of time and random alignment. The change of antenna gain in direction to each other can be modeled as the antenna mutual gain as described by ITU-R M.1372 [21]. By substituting the transmitter and receiver antenna gains for the mutual gain $MG(t)$, the equation becomes a function of time.

$$I(t) = P_T + MG(t) - L_T - L_R - L_P - FDR \tag{3}$$

In case that the radar systems and frequency bands are known, the L_P and $MG(t)$ are two major factors that affect the interference power level. Therefore, a simulation program to generate time-varying mutual gain $MG(t)$ for any radar beam-scanning scenarios with various propagation model L_P is developed and utilized in this paper. The objective of the simulation was to check whether the interference signal exceeded the power thresholds of IPCs for specific beam-scanning scenarios and analyze statistically.

Most standards and recommendations on radar interference provide IPCs for victim radar systems in terms of I/N, S/I, or S/(N+I), where I is the interference, N is the noise, and S is the signal. The effects on victim radar will vary based on the modulation type of interference signal and victim receiver. In this paper, we assume that the interference signal is received like wide band noise or CW, which will increase noise level. In reality, linear frequency modulated signals are more likely to be received by victim radar because of the compression gain. In this paper, we set the scope of the analysis to the worst-case interference signal, which is a high power CW interference signal is received for all receiver operating time. The effect of modulation and waveform of victim and interference signal will be investigated in the future work. Thus, to protect radar from interference, the interference signal should not exceed a certain power level relative to the receiver noise. In this study, we used

FIGURE 4. Examples of L and S band radars. (Left) Raytheon ASR-10SS, (Right) Indra PSR.

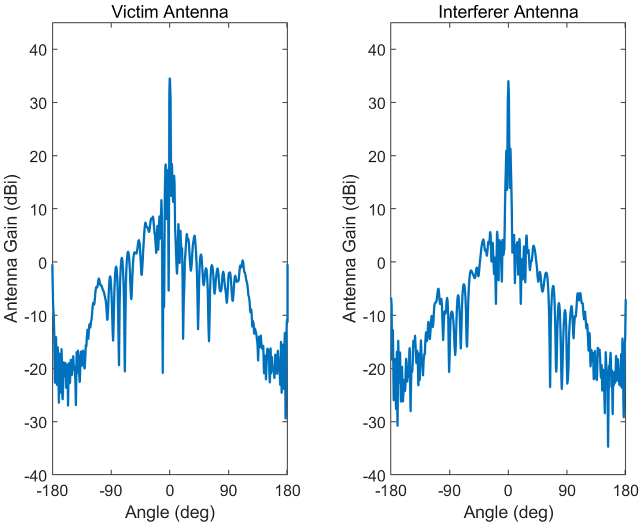

FIGURE 5. Far-field radiation patterns of interferer and victim radars generated from EM simulation.

an IPC of I/N $= -6$ dB as in other literatures [8], [22]. An interference signal that exceeds an IPC will degrade the radar performance in terms of the maximum detection range or detection probability. The expected radar performance of radar with given SNR are presented in [23] and [24] and referred in below equation 4.

$$P_D = 0.5 \cdot erfc\left(\sqrt{-\ln P_{fa}} - \sqrt{\frac{SNR_{min}}{1+I/N} + 0.5}\right) \quad (4)$$

where $SNR_{\min}$ is the minimum required SNR, P_D is the detection probability, $erfc$ is the Gauss error function, and P_{fa} is the false alarm rate for the receiver of the victim radar.

B. INTERFERENCE SIMULATION

1) PROPOSED METHOD

In this section, we describe the proposed inter-radar interference simulation method, which is shown in Fig. 3. The simulation program represents the interference power at the victim receiver by following seven functional blocks. The first block works as initialize step, which sets and loads parameters based on specifications of the interferer and victim radars. The signal bandwidth, signal type, IPCs, noise figure, insertion losses, FDR, and maximum transmitted power of the interference signal are prepared for the analysis. The FDR was set to 0dB assuming the worst-case scenario. The 0dB FDR means that the interfering signal is directly received by the victim radar without RF filtering. As explained in section II, the path losses from propagation models are obtained by the radar locations.The radar beam-scanning scenarios are generated based on the antenna radiation patterns of the interferer and victim radars, the azimuth rotation speed, and the rotation area. In this study, we utilized the 3D radiation patterns of the Cassegrain and Gregorian antennas for electromagnetic simulation with gains of 38.1 dBi and 35 dBi, respectively. However, it is also possible to use the mathematical models for antenna radiation patterns recommended by ITU-R M.1851-1 [25]. The antenna radiation patterns of victim and interferer are converted to vector format based on the scenario input. The fourth block generates mutual gain with the radiation pattern vector. The random alignment between the interferer and victim radars, time and angle resolution are considered in this step. Based on the mutual gain, the interference power is calculated at the victim receiver by using equation 3. To further analysis, the interference power is converted to I/N, S/I, and S/(N+I) by using the victim radar parameters. Finally, the interference power is compared with the IPCs to check whether the interference signal exceeds the IPCs, and the statistics are visualized.

TABLE 3. The parameters of the interferer and victim radars for the analysis.

Victim		Interferer	
Item	Value (Unit)	Item	Value (Unit)
Antenna Gain	34.5 (dBi)	Antenna Gain	34 (dBi)
Bandwidth	5 (MHz)	Bandwidth	5(MHz)
System Losses	3 (dBm)	System Losses	3 (dBm)
Noise Figure	4 (dB)	Transmit Power	72.83 (dBm)
Rotation Speed	12 (RPM)	Rotation Speed	15 (RPM)
Minimum SNR	8 (dB)	FDR	0 (dB)

2) SIMULATION PARAMETERS AND SCENARIOS

We set the parameters of the interferer and victim radars according to the S band (2.8 GHz) used by airport primary surveillance radar (PSR). The parameters of the interferer and victim radars are referenced from [26] and [27] and summarized in Table 3. The pulse repetition frequency of the interferer radar was set to 1 kHz, which is synchronized to the time resolution as the analysis. Because there is no IPC for the recommended I/N of a pulsed radar, we temporarily compared the interference signal power with the victim receiver noise power based on an IPC of I/N $= -6$ dB. The analysis results are presented in Table 2 with the path loss from terrain case 1 and time percentage $p = 0.5$.

We assumed an azimuthal rotation for both the interferer and victim radars. Example radar beam-scanning scenarios used to simulate inter-radar interference are presented below. The two main categories were the rotation and sector, which are common operation scenarios for radiodetermination and radiolocation radars used in airport surveillance and weather.

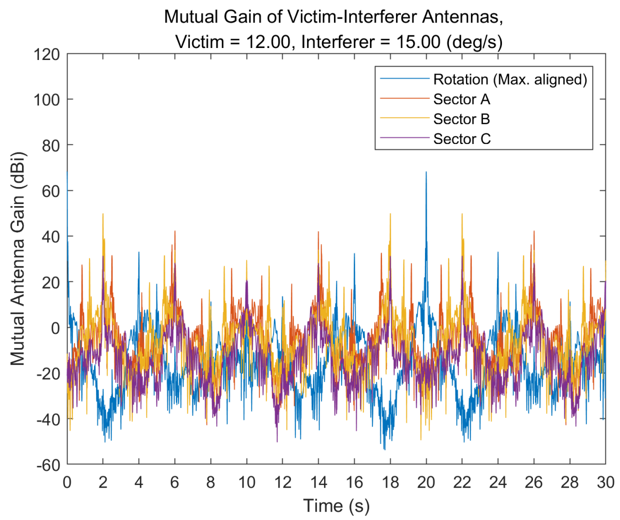

FIGURE 6. Time-domain mutual gain from different beam-scanning scenarios.

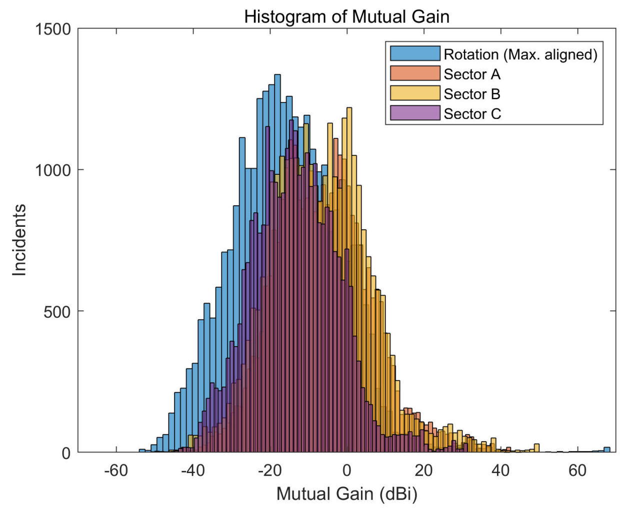

FIGURE 7. Histogram distribution of mutual gain for different beam-scanning scenarios.

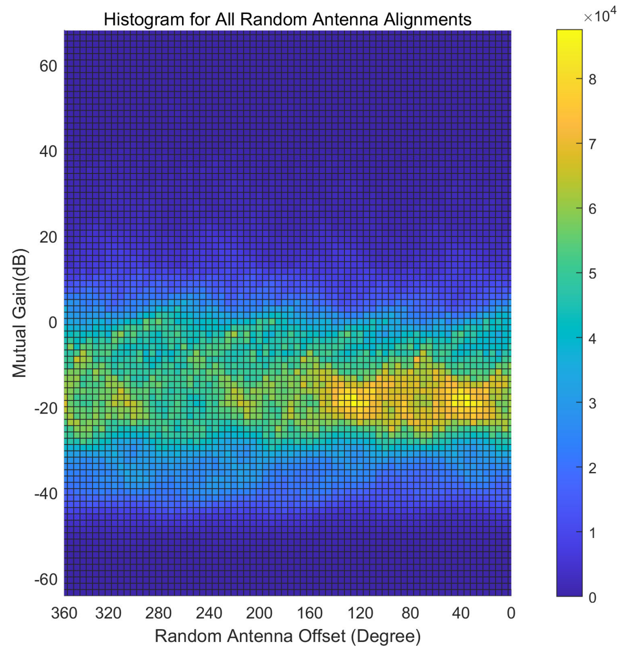

FIGURE 8. Histogram of the mutual gain for all random interferer antenna alignments in rotation scenarios.

The time-domain mutual gain $MG(t)$ of a radar scan is calculated as follows:

$$MG(t) = G_{Rx}(t \cdot \omega_{Rx}) + G_{Tx}(t \cdot \omega_{Tx} + \theta_{random}) \quad (5)$$

where G_{Rx} is the antenna gain, ω_{Rx} is the rotation speed of the victim radar, G_{Tx} and ω_{Tx} are the corresponding antenna gain and rotation speed, respectively, of the interferer radar, and θ_{random} is random angle difference between interferer and victim radar.

a: ROTATION SCENARIO

Both the interferer and victim radars rotated antennas on the azimuthal plane. The rotation direction was assumed as clockwise, but the rotation speed differed. The initial angle for the antenna of the interferer radar was randomly selected, and the initial angle for the antenna of the victim radar was set to zero.

b: SECTOR SCENARIO

The victim radar system rotated the antenna in a certain range, while the interferer rotated its antenna on the azimuthal plane. The sector scenarios were divided with respect to the maximum interference direction as detailed below. Both antennas were randomly aligned initially.

A. The center of the sector was in the same direction as the maximum interference direction.
B. The sector was not symmetric to the maximum interference direction, but the path was included in the sector.
C. The sector did not include the maximum interference direction.

C. RESULTS AND DISCUSSIONS

1) RADAR BEAM-SCANNING SCENARIO

Fig. 6 shows the time-domain mutual gain based on 30,000 data, which is equivalent to 30 s. The blue line represents the scenario where the victim and interferer are rotating but they are aligned initially. In this result, the theoretical maximum interference repeatedly occurs at t = 0, 20 s, 40 s.

To compare the differences in interference power among various scenarios, the average mutual gain was obtained for the rotation, sector A, sector B, and sector C scenarios: −15.4, −5.9, −6.7, and −15.5 dB, respectively. The two average gains for the rotation and sector C scenarios were similar, but the maximum interference power differed by 36.97 dB, which may exceed interference allowance level. The maximum value for the rotation scenario was 68.26 dB and that for the sector C scenario was 31.28 dB. Therefore, a comprehensive statistical analysis is required for both the

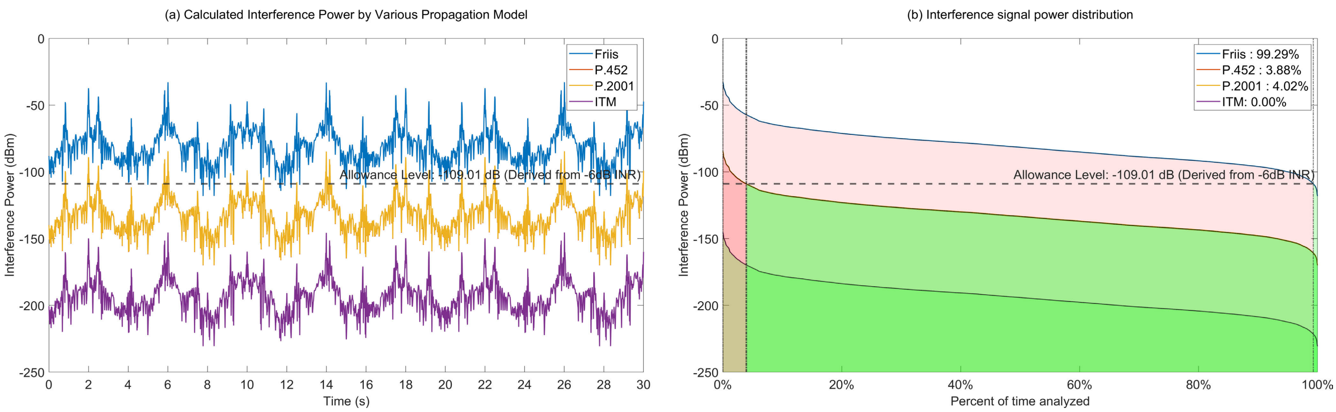

FIGURE 9. **Result of inter-radar interference analysis. Protection criteria is set to INR = −6 dB and converted to power level by victim radar specification. The beam scanning scenario is sector A and the locations of each radar is from terrain case 3.**

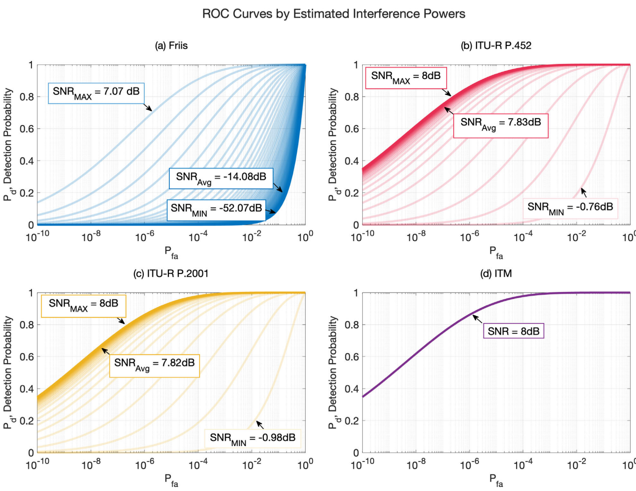

FIGURE 10. **The expected detection performance degradation of victim radar is presented as receiver operating characteristic (ROC) curve. The SNR of received signal without interference is supposed as 8 dB, 4 non-coherent pulse integration and non fluctuating targets are assumed. The interference signal above IPC is considered as noise, resulting lower SNR.**

maximum and average interference based on the proposed method.

All sector scenarios resulted in a short periodicity because of the narrow rotation angle. Thus, the mutual gains of the sector scenarios were focused in a certain range, as depicted in Fig. 7. In contrast, the mutual gain of the rotation scenario showed a wider distribution compared to the sector scenarios, but it could be changed by the initial random antenna alignment.

To analyze the differences in mutual gain caused by random alignment, the mutual gain of the rotation scenario was simulated for every possible random angle. Fig. 8 shows the mutual gain vs. random antenna offset at the start of the rotation scenario. The color of the pixel represents the number of times for the predicted mutual gain in a particular scenario. The incident number of the main beam alignment under 1 degree was calculated as 1974 from a total of 1.08×10^8 data, which means that the probability was 1.82×10^{-5}. By extending the worst-case scenario of the main beam alignment to a mutual gain above 60 dB, the incident number became 24,264 and the probability was 2.24×10^{-4}. The incident number at a mutual gain below 0 dB was 94,664,238, which is 87.6% of the total time. Therefore, considering all possible random alignments between the two radars, the probability of the main beam alignment was less than 0.01% for the presented rotation scenario. With the above analysis, the proposed method can be used to derive a probability threshold in time.

2) PROPAGATION MODEL

Figure 9. presents interference analysis results for the NLOS case, terrain case 3 and sector A scenario. First, the time-domain mutual gain is calculated as in Fig. 9(a) and used to determine the interference power and its effect on the victim radar for 4 different propagation models. For a given IPC and receiver specification, the allowance power level is derived and compared with the time varying interference power due to beam scanning scenario, as depicted in Fig. 9(b). The proposed analysis allows us to calculate the exact time and duration for which the interference power exceeds the threshold.

In Fig. 9, the yellow solid line represents analysis result with P.2001 propagation model. The basic radar performance, maximum radar detection range and detection probability, decreased significantly when the interference signal exceeded the allowed level. With the proposed method, the time percentage for radar performance degradation can be estimated as 3.7% of the total operation time and this may significant to the victim radar. In contrast, a different propagation model ITM will led to dramatically different results and conclusions with same radar system and environment. ITM presented a greater path loss than ITU-R P.452 and P.2001 because of diffraction as described in section II, and the analysis result shows that there will be no interference between the radars as presented in Fig. 9 (b). The Friis model expected a 99% interference time, however, this is not appropriate analysis for the NLOS scenario. Therefore, the selection and

TABLE 4. Comparison of related studies and the proposed analyzes.

Reference	Year	Analysis Results	Frequency	Scanning Scenario	Propagation Model	Notes
[18]	2022	Interference power, SNR, Time series interference	5600 MHz	Precipitation, Volume Scan	Friis (Free space)	Measured results. Synchronized scan showed minimum interference for the weather radar network.
[19]	2021	Bistatic power, SNR (in azimuth plane)	88,91,105 MHz	Fixed, Three locations	Friis (Free space)	Measured results are provided. Bistatic passive radar performance analysis.
[4]	2019	Interference power	2600 MHz	Fixed	ITU-R P.452	Inband and out-of-band analysis
[8]	2019	Interference power, FDR, Guard band	3300 MHz	Fixed	ITU-R P.452	OFDM waveforms, filtering and windows are suggested.
[10]	2019	Interference power	3650 MHz	Fixed	ITM	Omnidirectional antenna assumed.
[14]	2018	Interference power, SNR, Data Throughput	3600 MHz	Rotation (30/60 RPM)	Friis (Free space)	Antenna backlobe is assumed to be -60 dB. Interference results are presented as "rare event".
[13]	2017	Interference power, Protection radius	2900 MHz	Fixed	Extended Hata	Omnidirectional antenna assumed.
[11]	2016	Interference power	3500 MHz	Fixed	Unknown	Two propagation losses in opposite directions.
[15]	2015	Probability of detection	L and S band	Fixed	Unknown	Two type of interference signals are analyzed. (LFM/LTE). The required SNR from target is presented.
This work	2022	Interference power & Time	L and S band	Rotation, Sector Scan	ITU-R P.452, ITU-R P.2001, ITM	Interference power, duration and probability are presented.

understanding of the propagation model is important for the interference analysis.

The proposed method predicted the expected performance degradation of the victim radar as a receiver operating characteristic (ROC) curve, in the Fig. 10. The SNR of victim radar is assumed to be 8 dB and the interference power is considered as additional noise source of the victim radar. The ROC curve is a graphical representation of the performance of a detection or binary classifier system, as its discrimination threshold is varied. It is obtained by 150 quantiles of calculated signal to noise ratio (SNR), and the transparency of each curve represents the number of times of the SNR value. Thus, curves with distinct colors mean radar performance expected for most of the time.

In Fig. 10 (a), a large number of SNR values are observed at less than -14 dB, which means that the interference power is dominant, and targets are hardly detected. On the other hand, in case of (b) and (c), the most of SNR values are near 8 dB and the victim radar rarely experiences interference. As previously analyzed in Fig. 9, the estimated radar performance from ITM model in Fig. 10 (d) is consistent.

These analysis results can be utilize to minimize the interference time amount or power, to determine beam-scanning scenario or interference mitigation methods. If the interference power is not enough to damage the victim radar with no performance degradation as calculated in ITM model, the operator may not need any modifications on the radar system. In case of Fig. 9 with ITU-R P.452 and P.2001 model, the victim radar may consider frequency hopping for certain radar scan sector or time window. This performance estimation has a limitation that the interference power is added up to the victim radar noise power. The actual performance degradation will be determined by the radar receiver structure and signal processing.

3) DISCUSSIONS

The most important purpose of this paper is radar interference analysis. Therefore, the propagation path loss model used as the ingredient for the interference analysis must be highly reliable. The propagation models we used are, in particular, ITU-R P.452, ITU-R P. 2001, and ITM-Longley Rice three models, because all of these models have been verified for their reliability at the measurement level [5], [6], [7], [8], [9], [10], [11], [12], and [13].

Our interference analysis method can be applied regardless of various frequency bands and radar classifications as long as the constraints in table 1 of the radio wave model are guaranteed. The reason that the analysis was limited to S-band and L-band radars is that the analysis target of our study is the interferometric analysis of weather and airport main surveillance radars used by civilians. These radars mainly use the S and L bands.

The target of propagation path loss analysis in this paper is limited to the topography of Korea. However, this limitation is only a matter which we intend to analyze. Basically, the three radio models we use are designed to be applied to the world's topography. In addition, the Korean topography is mostly mountainous, and various multi-paths can be created. All three models return a single propagation path loss value considering these multi-paths. Therefore, there is a limitation that multi-path fading cannot be considered concretely. However, since our analysis is based on interference analysis, the worst-case analysis is fundamentally important. In terms of interference, fading has an effect of suppressing interference, so it is not required to consider it in our analysis.

We compared the proposed method with the other interference analysis literatures in Table 4. As shown in the table, every interference analysis starts from the calculation of interference power to the victim radar. In same manner, the proposed method is the first step of the interference analysis, not the whole process. This study presents a method to select proper propagation models and compare different radar scan scenario for the interference analysis.

The radar system receives signal from the environment and process the signal with various algorithms and processes. The modulation, timing, receiver structure and signal processing will mitigate the interference and the output from radar system may different from this analysis. By providing interference power and probability distribution in given environment, the radar system designer and operator can consider the interference mitigation methods and the radar system performance degradation.

Therefore, the future work will focus on the analysis of the radar system performance degradation based on given interference power. For example, the L and S band radar commonly uses two type of pulses, short pulse for close range detection and long pulse for wide coverage. The short pulse is not modulated, but the long pulse is linearly modulated in frequency domain. The modulation will affect the victim radar in different ways. Also, commonly used radar techniques such as pulse repetition frequency dithering, carrier frequency diversity, sensitivity time control, integration, detection, and tracking will mitigate one-time interference. Also, system ambiguity can be another consideration for the interference analysis.

IV. CONCLUSION

This paper studies the comparative inter-radar interference analysis method with propagation models and beam scanning scenarios for L and S bands. The selection of different propagation models and statistical input parameters can result in significant differences in the calculated path loss, which can affect the interference probability and conclusions of the analysis. Based on the scenario and parameters in this paper, ITU-R P.452 and P.2001 is recommended for estimating the worst-case interference, and ITU-R P.2001 is recommended for cases with high time percentages, such as interference from CW-like transmitted signals. ITM is recommended for estimating the average interference of NLOS cases with complex and irregular terrain. Simulation analyses for common beam-scanning scenarios, rotation and sector scans, showed that interference levels and probabilities are changing by the scenario significantly. The maximum possible interference probability was calculated as 1.82×10^{-5} when both radars were rotating at fixed and different rotation speeds. Based on the proposed method, the time, duration and power of interference can be derived and statistically analyzed in a given radar system and beam-scanning scenario. The proposed results can help to select interference mitigation methods or to determine beam-scanning area and radar parameters.

The presented method can be extended by in-depth radar simulation considering receiver structure, system ambiguity, matched filtering, signal processing and interference mitigation techniques. With the future work, precise interference analysis can be performed, and the spectrum efficiency will be improved for L and S band radars.

REFERENCES

[1] *Procedures for Determining the Potential for Interference Between Radars Operating in the Radiodetermination Service and Systems in Other Services*, ITU Radiocommunication M.1461-2, 2018.
[2] *Theoretical Analysis and Testing Results Pertaining to the Determination of Relevant Interference Protection Criteria of Ground-Based Meteorological Radars*, ITU Radiocommunication M.2136, 2008.
[3] *Technical and Operational Aspects of Ground-Based Meteorological Radars*, ITU Radiocommunication M.1849-2, 2019.
[4] N. Moraitis and K. S. Nikita, "Interference analysis between LTE-2600 MHz networks and air traffic control radars in S-band," in *Proc. 13th Eur. Conf. Antennas Propag. (EuCAP)*, 2019, pp. 1–5.
[5] J. H. Kim, J. H. Oh, and Y. J. Chong, "Measurement of anomalous propagation in the south seashore of Korea," in *Proc. Int. Symp. Antennas Propag. (ISAP)*, 2018, pp. 1–2.
[6] M. Kvicera, P. Pechac, M. Grabner, V. Kvicera, P. Valtr, and A. Martellucci, "Experimental study on terrestrial links enhancement at 11 and 38 GHz," *IEEE Trans. Antennas Propag.*, vol. 63, no. 7, pp. 3179–3186, Jul. 2015.
[7] M. Kvicera, T. Korinek, V. Kvicera, M. Grabner, P. Valtr, P. Pechac, and A. Martellucci, "Short-term terrain diffraction measurements from L-to Q-band: Results and analysis," *IEEE Trans. Antennas Propag.*, vol. 62, no. 7, pp. 3693–3701, Jul. 2014.
[8] J. Park, E. Lee, S.-H. Park, S.-S. Raymond, S. Pyo, and H.-S. Jo, "Modeling and analysis on radio interference of OFDM waveforms for coexistence study," *IEEE Access*, vol. 7, pp. 35132–35147, 2019.
[9] M. Kvicera, P. Pechac, P. Valtr, T. Korinek, V. Kvicera, M. Grabner, and A. Martellucci, "Influence of input terrain profile resolution on diffraction modeling," *IEEE Antennas Wireless Propag. Lett.*, vol. 14, pp. 1318–1321, 2015.
[10] T. T. Nguyen, A. Sahoo, and T. A. Hall, "A practical approach to placing coastal sensors for spectrum sharing in the 3.5 GHz band," in *Proc. IEEE Wireless Commun. Netw. Conf. (WCNC)*, Apr. 2019, pp. 1–7.
[11] F. H. Sanders, E. F. Drocella, and R. L. Sole, "Using on-shore detected radar signal power for interference protection of off-shore radar receivers," Nat. Telecommun. Inf. Admin. (NTIA), Washington, DC, USA, Tech. Rep. TR-16-521, 2016.
[12] N. N. Krishnan, R. Kumbhkar, N. B. Mandayam, I. Seskar, and S. Kompella, "How close can i be?—A comprehensive analysis of cellular interference on ATC radar," in *Proc. IEEE Global Commun. Conf. (GLOBECOM)*, Dec. 2017, pp. 1–6.
[13] N. N. Krishnan, R. Kumbhkar, N. B. Mandayam, I. Seskar, and S. Kompella, "Coexistence of radar and communication systems in CBRS bands through downlink power control," in *Proc. IEEE Mil. Commun. Conf. (MILCOM)*, Oct. 2017, pp. 713–718.
[14] N. N. Krishnan, N. Mandayam, I. Seskar, and S. Kompella, "Experiment: Investigating feasibility of coexistence of LTE-U with a rotating radar in CBRS bands," in *Proc. IEEE 5G World Forum (5GWF)*, Jul. 2018, pp. 65–70.
[15] S. Kodituwakku, T. Lamahewa, and T. Dissanayake, "Impact on radar probability of detection due to interference from 4G communication signals," in *Proc. IEEE Global Electromagn. Compat. Conf. (GEMCCON)*, Nov. 2015, pp. 1–5.
[16] B. D. Cordill, S. A. Seguin, and L. Cohen, "Electromagnetic interference to radar receivers due to in-band OFDM communications systems," in *Proc. IEEE Int. Symp. Electromagn. Compat.*, Aug. 2013, pp. 72–75.
[17] G. Galati and G. Pavan, "Mutual interference problems related to the evolution of marine radars," in *Proc. IEEE 18th Int. Conf. Intell. Transp. Syst.*, Sep. 2015, pp. 1785–1790.
[18] M. Frech, C. Hald, M. Schaper, B. Lange, and B. Rohrdantz, "Assessing and mitigating the radar–radar interference in the German c-band weather radar network," *EGUsphere*, vol. 2022, pp. 1–21, Jun. 2022.
[19] M. Malanowski, M. Żywek, M. Płotka, and K. Kulpa, "Passive bistatic radar detection performance prediction considering antenna patterns and propagation effects," *IEEE Trans. Geosci. Remote Sens.*, vol. 60, pp. 1–16, 2022.
[20] *Frequency and Distance Separations*, ITU Radiocommunication Sm. 337-6, 2008.
[21] *Efficient Use of the Radio Spectrum by Radar Stations in the Radiodetermination Service*, ITU Radiocommunication M.1372-1, 2003.

[22] G. Jiang, Y. Fan, H. Yuan, and P. Yuan, "A method for the analysis of interference from DME to ATCRBS in the time domain," *Electronics*, vol. 8, no. 4, p. 393, Apr. 2019.
[23] D. Luong, B. Balaji, and S. Rajan, "Performance prediction for coherent noise radars using the correlation coefficient," *IEEE Access*, vol. 10, pp. 8627–8633, 2022.
[24] J. Candy and E. Breitfeller, "Receiver operating characteristic (ROC) curves: An analysis tool for detection performance," Lawrence Livermore National Lab. (LLNL), Livermore, CA, USA, Tech. Rep. LLNL-TR-642693, 2013.
[25] *Mathematical Models for Radiodetermination Radar Systems Antenna Patterns for Use in Interference Analyses*, ITU Radiocommunication M.1851-1, 2018.
[26] J. Groot, "Analysis of an emitter location algorithm for use in ESM systems," Tno Defence Security and Safety The Hague, The Netherlands, Tech. Rep. ADA452783, 2005.
[27] Indra. (2009). *Air Traffic Management Primary Surveillance Radar*. [Online]. Available: https://www.indracompany.com/sites/default/files/12_psr_brochure_v1_02-2009_eng.pdf

HYUNGJUNG KIM received the B.S. and M.S. degrees in electronics engineering from Hanyang University, Seoul, South Korea, in 1992 and 1994, respectively, and the Ph.D. degree in information communication engineering from the University of Chungbuk, Cheongju, Republic of Korea, in 2010. Since 1995, he has been with the Electronics and Telecommunications Research Institute, Daejeon, South Korea. He has conducted research on wireless communication systems and digital-RF. His current research interests include spectrum engineering and radar engineering.

YOUNGDAM KIM was born in Suwon, South Korea, in 1988. He received the B.S. degree in electronics engineering from Ajou University, Suwon, in 2011, and the M.S. and Ph.D. degrees in electrical engineering from the Korea Advanced Institute of Science and Technology (KAIST), Daejeon, South Korea, in 2013 and 2017, respectively. He worked as a Senior Engineer at Samsung Electronics Network Business, Suwon, in 2017. He worked as a Postdoctoral Researcher at KAIST, in 2018. He worked as a Senior Researcher at Agency for Defense Development (ADD), South Korea, from 2019 to 2020. He is currently an Assistant Professor with the Department of Electronics Engineering, Chungnam National University (CNU), Daejeon. His current research interests include the analysis of active phased antenna array and electromagnetic scattering problems based on applied computational electromagnetics.

MINSOO KANG received the B.S. and M.S. degrees in electrics engineering from Sogang University, Seoul, Republic of Korea, in 1996 and 1998, respectively, and the Ph.D. degree in electronics engineering from Chungnam National University, Daejeon, Republic of Korea, in 2011. From 1998 to 2000, he was with Hyundai Electronics Industry Company, Icheon, Republic of Korea, where he developed RF transceivers of base stations for mobile communication. In 2000, he joined ETRI, Daejeon, and works with the Radio and Satellite Research Division as a Principal Member of the Researching Staff. His current research interests include radar systems and spectrum engineering.

SANGIN CHO received the B.S. and M.S. degrees in information and telecommunication engineering from Chonbuk National University, South Korea, in 1997, and 1999, respectively. Since 1999, he has been with the Electronics and Telecommunications Research Institute (ETRI), Daejeon, South Korea. His current research interests include radio signal processing and radio management with applications to radar systems.

BYUNGKWAN KIM (Member, IEEE) received the B.S. degree in information and communication engineering and the M.S. and Ph.D. degrees in electrical engineering from the Korea Advanced Institute of Science and Technology (KAIST), Daejeon, Republic of Korea, in 2010, 2012, and 2017, respectively. In 2017, he joined the Samsung Advanced Institute of Technology as a Senior Researcher, Suwon, until February 2020. He is currently an Assistant Professor with the Department of Radio and Information Communications Engineering, Chungnam National University, Daejeon, South Korea. His current research interests include mmWave radar system design and radar signal processing with machine learning.